

Synergy between parthenolide and arsenic trioxide in adult T-cell leukemia/lymphoma cells *in vitro*

Hamideh Kouhpaikar¹, Mohammad Hadi Sadeghian¹, Houshang Rafatpanah², Mohaddeseh Kazemi², Mehrdad Iranshahi³, Zahra Delbari², Faezeh Khodadadi¹, Hossein Ayatollahi¹, Fatemeh B. Rassouli^{4*}

¹ Cancer Molecular Pathology Research Center, Department of Hematology and Blood Bank, Faculty of Medicine, Mashhad University of Medical Sciences, Mashhad, Iran

² Inflammation and Inflammatory Diseases Research Center, Faculty of Medicine, Mashhad University of Medical Sciences, Mashhad, Iran

³ Department of Pharmacognosy and Biotechnology, Biotechnology Research Center, Faculty of Pharmacy, Mashhad University of Medical Sciences, Mashhad, Iran

⁴ Novel Diagnostics and Therapeutics Research Group, Institute of Biotechnology, Ferdowsi University of Mashhad, Mashhad, Iran

ARTICLE INFO

Article type:
Original article

Article history:
Received: May 25, 2019
Accepted: Nov 13, 2019

Keywords:
Adult T-cell Leukemia/
Lymphoma
Arsenic trioxide
In vitro
Parthenolide
PCR

ABSTRACT

Objective(s): Adult T-cell leukemia/lymphoma (ATLL) is an aggressive lymphoid malignancy with low survival rate and distinct geographical distribution. In search for novel chemotherapeutics against ATLL, we investigated the combinatorial effects of parthenolide, a sesquiterpene lactone with valuable pharmaceutical activities, and arsenic trioxide (ATO) *in vitro*.

Materials and Methods: MT2 cells, an ATLL cell line, were treated with increasing concentrations of parthenolide (1.25, 2.5, and 5 µg/ml) and ATO (2, 4, 8, and 16 µM) to determine their IC₅₀. Then, cells were treated with a combination of sub-IC₅₀ concentrations of parthenolide (1 µg/ml) and ATO (2 µM) for 72 hr. Cell viability and cell cycle changes were assessed by Alamar blue and PI staining, respectively. To understand the mechanisms responsible for observed effects, expression of *CD44*, *NF-κB (REL-A)*, *BMI-1*, and *C-MYC* were investigated by real-time PCR.

Results: Assessment of cell viability indicated that parthenolide significantly increased the toxicity of ATO, as confirmed by accumulation of MT2 cells in the sub G1 phase of the cell cycle. Moreover, molecular analysis revealed significant down-regulation of *CD44*, *NF-κB (REL-A)*, *BMI-1*, and *C-MYC* upon combinatorial administration of parthenolide and ATO in comparison with relevant controls.

Conclusion: Taken together, present results showed that parthenolide significantly enhanced the toxicity of ATO in MT2 cells. Therefore, the future possible clinical impact of our study could be combinatorial use of parthenolide and ATO as a novel and more effective approach for ATLL.

► Please cite this article as:

Kouhpaikar H, Sadeghian MH, Rafatpanah H, Kazemi M, Iranshahi M, Delbari Z, Khodadadi F, Ayatollahi H, Rassouli FB. Synergy between parthenolide and arsenic trioxide in adult T-cell leukemia/lymphoma cells *in vitro*. Iran J Basic Med Sci 2020; 23:616-622. doi: 10.22038/ijbms.2020.40650.9610

Introduction

Adult T-cell leukemia/lymphoma (ATLL) is an uncommon and aggressive lymphoid malignancy that is associated with human T-cell leukemia virus type 1 (HTLV-1). It has been estimated that 10–20 million people are infected with HTLV-1, and endemic regions include Central Africa, South America, the Caribbean basin, Iran, South-Western Japan, and Melanesia (1, 2). Among HTLV-1 infected patients, approximately 3–5% develop ATLL in four categories: acute (60%), lymphomatous (20%), chronic (15%), and smoldering (5%) types (3, 4).

In recent years, survival of ATLL patients has been improved by introduction of multiagent chemotherapy, antiviral therapies, and allogeneic hematopoietic stem cell transplantation, as well as advances in supportive care (5). Among all chemotherapeutic regimes, high response rates were observed after coadministration of interferon (IFN-α) and antiviral agent zidovudine, and also interferon-alfa (IFN-α) and arsenic trioxide (ATO), especially in the acute ATLL patients (6). Nevertheless, ATLL relapses in most cases partially due to intrinsic

drug resistance mediated by p-glycoprotein (p-gp) and anti-apoptotic proteins (7).

Parthenolide, first isolated from medicinal plant *Tanacetum parthenium*, is a sesquiterpene lactone of the germacranolide class with a wide range of pharmaceutical activities such as anti-inflammatory and anti-cancer effects (8, 9). Parthenolide contains an alpha-methylene-gamma-lactone ring through which it interacts with nucleophilic sites of multiple biological targets and induces its various effects. Low solubility of parthenolide in water is a physico-chemical property that limits biological applications of this compound. However, a new approach has been proposed for synthesis of parthenolide derivatives with better solubility and higher potency (10). *In vitro* studies demonstrated anti-proliferative activity of parthenolide in the prostate, pancreatic and colorectal cancer cells (11–13), and also multiple myeloma and acute myelogenous leukemia cells (14). In addition, synergistic effects of parthenolide and chemotherapy drugs have been reported in breast carcinoma and colorectal adenocarcinoma cells (15, 16). Suppression of

Nuclear factor kappa beta (NF κ B) and Signal transducer and activator of transcription 3 (STAT3) signaling pathways, inhibition of A mitogen-activated protein kinase (MAPK) activity and induction of mitochondrial dysfunction are a number of mechanisms introduced for parthenolide anticancer effects (9).

Poor outcome of current chemotherapy modalities in ATLL has made it crucial to investigate novel approaches with higher efficacy. Although anticancer and synergic effects of parthenolide have been demonstrated in various cell types, pharmaceutical effects of parthenolide, alone or in combination with other chemicals, have not as yet been reported in ATLL. Accordingly, we investigated whether combination of parthenolide with ATO could improve cytotoxicity in HTLV-1-infected cells. In this regard, cell viability was assessed using Alamar blue, cell cycle was analyzed by PI staining and flowcytometry, and expression patterns of CD44, *NF- κ B* (*REL-A*), BMI-1, and *C-MYC* were investigated by real-time polymerase chain reaction (PCR).

Materials and Methods

Chemicals and reagents

Parthenolide was obtained from Euroasia (China). ATO, Alamar blue, and propidium iodide (PI) were purchased from Sigma Aldrich (Germany). Dimethylsulfoxide (DMSO) and Triton X-100 were from Merck (Germany). RPMI 1640 was obtained from Biosera (France) and Fetal Bovine Serum (FBS), penicillin/streptomycin, and L-glutamine were supplied by Gibco (Scotland). Tripure was from Roche (Germany) and M-MuLV reverse transcriptase was from Thermo Scientific (USA), while the SYBR green mix was purchased from Takara (Japan).

Cell treatment and viability assay

The MT-2 cell line (lymphoma cells infected with HTLV-I derived by co-cultivating normal human cord leukocytes and human leukemic T-cells) was donated by Inflammation and Inflammatory Diseases Research Center, Faculty of Medicine, Mashhad University of Medical Sciences (generous gift from Prof. Houshang Rafatpanah). MT2 cells were maintained in RPMI 1640 supplemented with 10% FBS, 1% (W/V) penicillin/streptomycin, and 1% L-glutamine, and incubated at 37 °C in 5% CO₂. To prepare different concentrations of parthenolide, 2 mg of the crystal was dissolved in 100 μ l DMSO and diluted with complete culture medium, while equal amount of DMSO in all parthenolide concentrations (0.2% v/v) was considered as the control treatment. Half

maximal inhibitory concentration (IC₅₀) of parthenolide and ATO were determined upon treatment of MT2 cells (5 \times 10⁴ cells/well) with increasing concentrations of parthenolide (1, 2.5, and 5 μ g/ml) and ATO (2, 4, 8, and 16 μ M) for 24, 48, and 72 hr. Then, cells were treated with a combination of sub-IC₅₀ concentrations of parthenolide (0.5, 0.75, and 1 μ g/ml) and ATO (0.5, 1, and 2 μ M) for 72 hr.

To assess the viability of cells, Alamar blue (0.1 mg/ml) was added (20 μ l/well) by the end of each time point and cells were incubated at 37 °C for 2 hr. Then, absorbance was measured at 600 nm using a microplate reader (Epoch, USA) and cell viability (%) was calculated using the following equation: 100-((AT-AU)/(AB-AU) \times 100), in which AT and AU were absorbance of treated and untreated cells, respectively, and AB was absorbance of blank control.

To determine drug interactions in our combinatorial treatment, the Combination Index (CI) was calculated, which evaluates synergism or antagonism between drugs; A value of CI > 1 means antagonism, CI = 1 shows additive, and CI < 1 indicates synergism (17).

Cell cycle analysis

Changes induced in the cell cycle after combinatorial use of parthenolide and ATO were studied after PI staining. Briefly, MT2 cells in each treatment were collected and washed with cold PBS containing 5% FBS. Then, cell pellets were resuspended in a hypotonic buffer containing 100 μ g/ml PI, 0.1% sodium citrate, and 0.1% Triton X-100, incubated for 30 min at 37 °C in the dark, and analyzed by flowcytometry (BD FACSCalibur) using FL2 filter.

Gene expression studies

Real-time PCR was performed to study the expression pattern of four candidate genes upon coadministration of parthenolide and ATO. To do so, at first the total cellular RNA was extracted from treated cells and their relevant controls using Tripure (Roche, Germany) followed by synthesis of cDNAs by random hexamer, dNTPs, and M-MuLV reverse transcriptase according to the manufacturer's protocol. Real-time PCR was conducted in Rotor-Gene 6000 detection system (Qiagen, Germany) using the SYBR green mix and primers listed in Table 1 for CD44, BMI-1, and *C-MYC* genes, while a TaqMan probe and specific primers were used for *NF- κ B* (*REL-A*). In all analyses, beta-2 microglobulin transcripts were considered as the internal control. PCR cycling conditions were 94 °C for 2 min, [94 °C for 15 sec, 60 °C

Table 1. List of primers, their sequence, and product length used for the real-time PCR analysis in current study

Gene name	Sequence (5'→3')	Accession number	Product length bp
β_2M	Forward: AATTGAAAAGTGGAGCATTGAGA Reverse: GGCTGTGACAAAAGTCACATGGTT	NM_004048.3	127
β_2M	Forward: TTGTCTTTTCAGCAAGGACTGG Reverse: CCACTTAACTATCTTGGGCTGTG Probe: TCACATGGTTTCACACGGCAGGCAT	NM_004048.3	127
<i>REL-A</i>	Forward: ACCCCTTCCAAGTTCCTATAGAAGAG Reverse: CGATTGTCAAAGATGGGATGAGAAAG Probe: ACTACGACCTGAATGCTGTGCGGCTCT	XM_011545206.2	145
<i>BMI-1</i>	Forward: CTGCAGCTCGCTTCAAGATG Reverse: CACACACATCAGGTGGGGAT	NM_005180.8	192
<i>C-MYC</i>	Forward: ACTCTGAGGAGGAACAAGAA Reverse: TGGAGACGTGGCACCTCTT	NM_002467.5	159
<i>CD44</i>	Forward: CGGACACCATGGACAAGTTT Reverse: GAAAGCCTTCAGAGGTCAG	XM_006718390.4	176

for 30 sec, 72 °C for 30 sec] (40 cycles) for CD44, BMI-1, and *C-MYC*, and 95 °C for 2 min, [95 °C for 15 sec, 60 °C for 30 sec, 72 °C for 30 sec] (45 cycles) for *NF-κB (REL-A)*.

Statistical analysis

The statistical significance was assessed by one way ANOVA and Tukey multiple comparisons test using Graph pad prism version 6.07 and SPSS version 16. In addition, CI was calculated using the Compusyn software package and results of flowcytometry were analyzed by Win-MDI version 2.8. All data were presented as mean ± SD and *P*-values less than 0.05, 0.001, and 0.0001 were considered significant for all comparisons.

Results

Inhibitory effects of parthenolide and ATO on the viability of MT-2 cells

As indicated in Figures 1 A and B, parthenolide and ATO did not induce significant toxic effects on MT2 cells after 24 hr. Nevertheless, 48 hr after treatment of cells with the highest concentrations of each agent, a significant decrease in cell viability was detected. However, IC₅₀ of parthenolide and ATO was only determined after 72 hr, which was 5 µg/ml for parthenolide and >16 µM for ATO. To note, cells treated with 0.2% DMSO were considered as relevant control for all treatments including parthenolide.

Combination of parthenolide and ATO induced more toxic effects on MT2 cells

After determination of IC₅₀ values, we investigated the combinatorial effects of parthenolide and ATO. In this regard, cells were treated for 72 hr with parthenolide and ATO alone and combination in concentrations lower than their IC₅₀. Reduction in the cell viability after combination of parthenolide and ATO was significantly greater than that for parthenolide and ATO alone (0.001). As shown in Figure 1C, cytotoxicity of 2 µM ATO was increased by 1 µg/ml parthenolide up to 26.5%. CI values (Table 2) also indicated synergistic effects in different combinations of parthenolide and ATO.

Combination of parthenolide and ATO induced cell cycle changes

To determine whether combinatorial treatment of cells with parthenolide and ATO was associated with cell cycle changes, DNA content of MT2 cells was analyzed by flowcytometry. As presented in Figure 2, in untreated MT2 cells and cells treated with parthenolide and its relevant DMSO control 9%, 6.3%, and 8.1% of cells were detected in the sub G₁ phase of the cell cycle, respectively. However, this amount increased up to 21.5% after ATO administration. Moreover, upon combinatorial treatment with parthenolide and ATO, 31.6% of cells were presented in the sub G₁ phase, which was higher than that in DMSO and ATO treatment (15.1%).

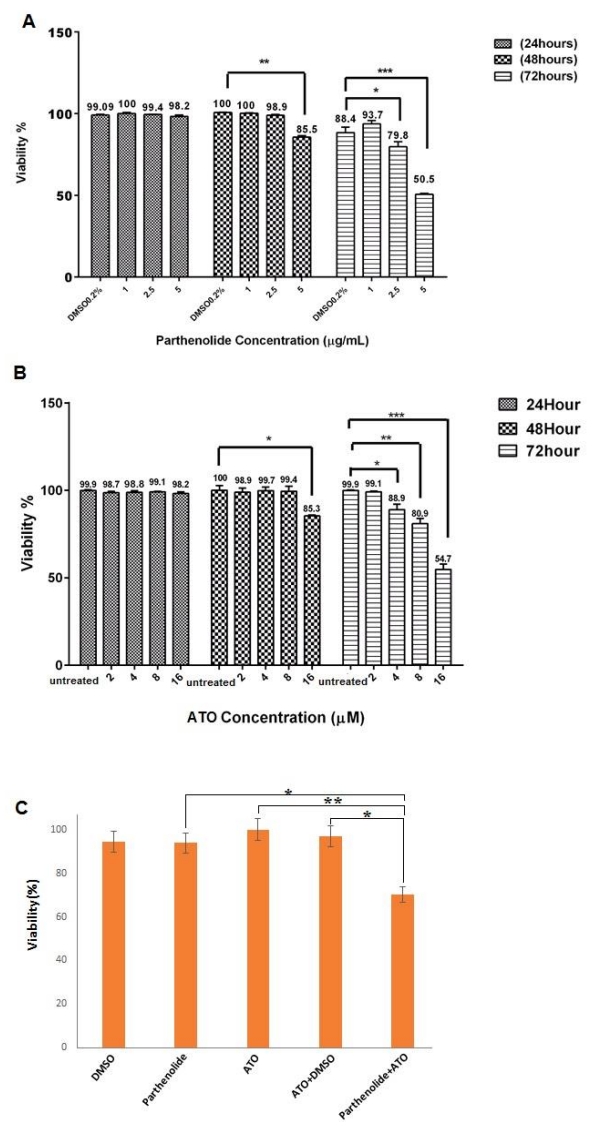


Figure 1. Cytotoxicity of parthenolide and ATO, alone or in combination, in MT2 cells. Cells were treated with various concentrations of parthenolide for 24, 48, and 72 hr, and IC₅₀ of parthenolide was determined as 5 µg/ml after 72 hr (A). After treatment of MT-2 cells with various concentrations of ATO for 24, 48, and 72 hr, its IC₅₀ was determined as >16 µM (B). Combinatorial use of parthenolide and ATO significantly reduced cell viability in comparison with other treatments (C)

Parthenolide and ATO decreased CD44, NF-κB (REL-A), and BMI-1 expression

To unravel molecular mechanisms underlying the combinatorial effects of parthenolide and ATO, expression patterns of CD44, *NF-κB (REL-A)*, BMI-1, and *C-MYC*, all of which contributed to proliferation and survival of ATLL cells, were studied by real-time PCR. As shown in Figure 3A, single-use of parthenolide and ATO significantly (*P*<0.0001) decreased CD44 expression

Table 2. CI values for parthenolide and ATO combination calculated for different concentrations

Parthenolide (µg/ml)	ATO (µM)	CI	Interpretation
0.5	1	0.79974	Synergism
0.75	1.5	0.80158	Synergism
1	2	0.71964	Synergism

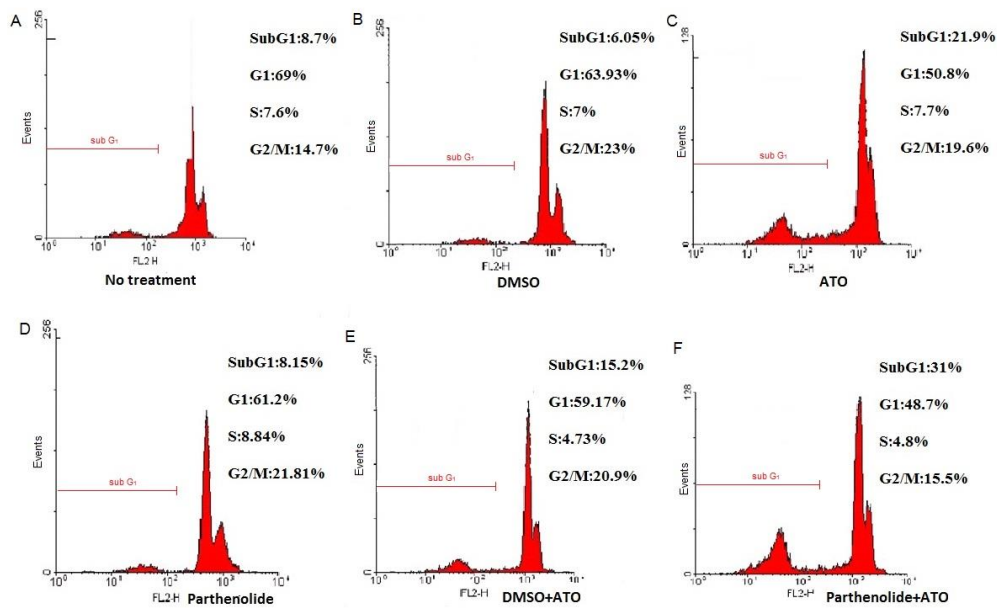


Figure 2. MT2 cell cycle analysis by PI staining. Untreated cells (A), cells treated with 0.2% DMSO (B), 2 μ M ATO (C), 1 μ g/ml parthenolide (D), 0.1% DMSO + 2 μ M ATO (E), and 1 μ g/ml parthenolide + 2 μ M ATO (F) for 72 hr. Sub-G1 peak, as an indicative of apoptotic cells, was specifically induced after parthenolide + ATO combination
 ATO: Arsenic trioxide; DMSO: Dimethyl sulfoxide

in comparison with their relevant controls. Moreover, combination of parthenolide and ATO induced negative regulatory effects on CD44 expression when compared with DMSO and ATO treatment. Studying *NF- κ B (REL-A)* expression revealed more interesting results; in comparison with relevant controls, parthenolide alone, but not ATO, significantly ($P < 0.05$) down-regulated *NF- κ B (REL-A)* expression and this effect was more considerable ($P < 0.001$) when combination of parthenolide and ATO was used (Figure 3B). Similar changes were observed when BMI-1 expression was

compared between each treatment and its relevant control. As presented in Figure 3C, single-use of parthenolide, quiet unlike ATO, significantly ($P < 0.001$) down-regulated BMI-1 expression, and intriguingly, combination of parthenolide and ATO decreased BMI-1 expression to lower levels ($P < 0.0001$). Nevertheless, analysis of *C-MYC* expression indicated a significant ($P < 0.001$) down-regulation upon ATO treatment, and such alteration was not observed after administration of parthenolide alone or in combination (Figure 3D).

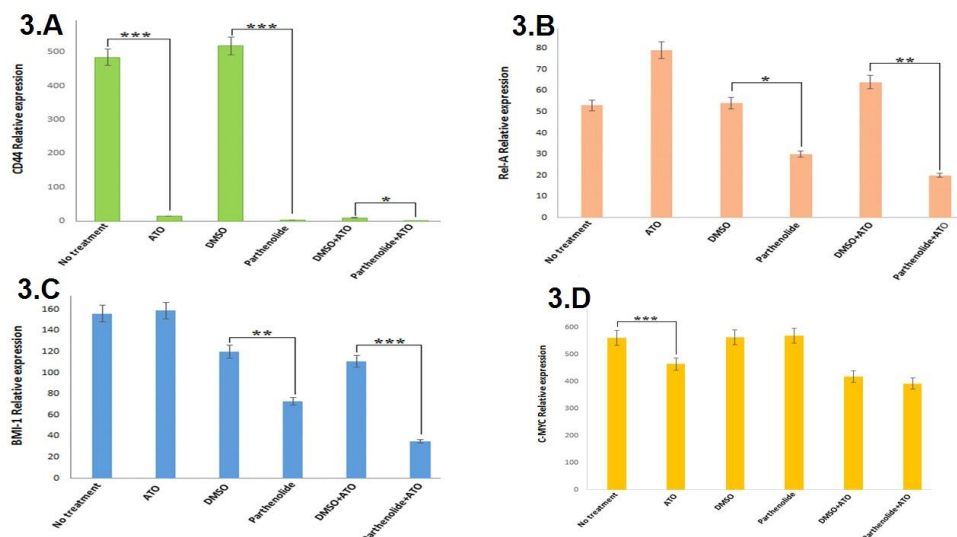


Figure 3. Real-time PCR analysis of CD44 (A), NF- κ B (REL-A) (B), BMI-1 (C), and C-MYC (D) expression 72 hr after treatment of MT2 cells with parthenolide and ATO, alone or in combination. To note, relative expression in each treatment was compared with its relevant control; ATO (2 μ M) with no treatment, parthenolide (1 μ g/ml) with DMSO (0.2%), parthenolide (1 μ g/ml) + ATO (2 μ M) with DMSO (0.1%) + ATO (2 μ M). * $P < 0.05$, ** $P < 0.001$, and *** $P < 0.0001$ compared with relevant controls
 ATO: Arsenic trioxide; DMSO: Dimethyl sulfoxide

Discussion

ATLL is an aggressive neoplasm of T-cells with serious complications in management and therapy, since resistance to conventional chemotherapeutics, both in the refractory stage and at the time of onset, is common among patients. Currently, designation of novel and more efficient combinatorial treatments is one of the main scopes in cancer research (18). The present study was carried out to investigate whether combination of parthenolide and ATO, a drug routinely prescribed for ATLL, could improve the efficacy of chemotherapy *in vitro*.

Parthenolide is a natural terpenoid derivative with valuable anticancer activities. In the current study, assessment of MT2 cell viability revealed enhanced toxicity of ATO when used in combination with non-toxic parthenolide. Although previous studies have shown improved cytotoxicity of anticancer drugs doxorubicin, 5-fluorouracil, paclitaxel, cisplatin, and taxol by parthenolide in melanoma and colorectal and lung cancers (16, 19-21), this is the first report on efficient combination of parthenolide and ATO in hematologic cancer cells. Observed synergy in our study might be partially due to inhibitory effects of parthenolide on p-gp, an efflux pump that mediates drug resistance in ATLL (18, 22).

Flowcytometry analysis revealed accumulation of MT2 cells in the sub G₁ phase of the cell cycle upon ATO treatment, alone and especially in combination with parthenolide. In line with our findings, it has been demonstrated that parthenolide, in combination with 5-fluorouracil or tumor necrosis factor (TNF)-related apoptosis-inducing ligand (TRAIL), induced sub G₁ arrest in colorectal cells (16, 23), similar to ATO that increased the proportion of myeloma cells in sub G₁ phase (24). Since down-regulation of cell cycle promoters, for example, *Cyclin D1*, has been attributed to inhibitory effects of parthenolide (25), induced alterations in the MT2 cell cycle could be explained by the decreased level of such proteins.

In the investigation of mechanisms involved in the synergy between parthenolide and ATO, expression of CD44, *NF-κB (REL-A)*, BMI-1, and *C-MYC* was analyzed by real-time PCR. CD44 is a transmembrane glycoprotein involved in metastasis and drug resistance of various cancer cell types (26). Overexpression of CD44 isoforms has been reported in hematopoietic malignancies such as non-Hodgkin's lymphoma, myeloma, and chronic and acute myeloid leukemia. CD44 expression is also associated with undesirable clinical prognosis in lymphoma and myeloma (27-29). In ATLL patients, enhanced expression of CD44 is correlated with disease severity, and HTLV-1 oncoprotein Tax is involved in this de-regulation (30). We observed significant down-regulation of CD44 upon single and combinatorial administration of parthenolide and ATO in ATLL cells. Previous studies have demonstrated that overexpression of CD44 in acute lymphoblastic leukemia cells enhanced drug efflux and promoted chemotherapy resistance (26). Therefore, the synergy between parthenolide and ATO might be partially due to the negative effects of both chemicals on CD44 expression.

Members of the *NF-κB* family are involved in critical biological processes such as cell survival, cell

cycle progression, and T-cell development (31, 32). In pathogenesis of ATLL, Tax activates *NF-κB* signaling, and thus, therapies that target the *NF-κB* pathway could induce apoptosis in ATLL cells (32). The negative effect of parthenolide on *NF-κB* expression has been previously reported in multiple myeloma and colon, gastric, and lung carcinoma cells (21, 33, 34). In addition, parthenolide in combination with balsalazide (prodrug of 5-aminosalicylate that reduces the risk of colon cancer in patients with ulcerative colitis) significantly suppressed nuclear translocation of *NF-κB* in colon cancer cells and further *in vivo* studies in the murine model showed that this combination inhibited carcinogenesis (35). Moreover, it has been shown that parthenolide in combination with sulindac synergistically inhibited cell growth in pancreatic carcinoma cells, and this combination reduced transcriptional activities and DNA binding of *NF-κB* (36). Similarly, our findings indicated a significant decrease in *NF-κB (REL-A)* expression by parthenolide, in single-use and also in combination with ATO. Since *NF-κB* promotes cell cycle by *Cyclins D1, D2, D3, and E* (37), decreased expression of *NF-κB (REL-A)* upon our combinatorial treatment could further explain sub G₁ accumulation of MT-2 cells.

BMI-1 is an oncoprotein involved in cell cycle regulation and cell immortalization, and its up-regulation has been reported in acute myeloid leukemia (AML) and lung, ovarian, nasopharyngeal, and breast carcinomas (38, 39). Several studies have revealed the involvement of BMI1 in tumor cell invasion in gastric, hepatocellular, pancreatic, and endometrial carcinomas, as well as the correlation between BMI-1 up-regulation and chemotherapy resistance (40). Furthermore, overexpression of BMI1 was associated with drug resistance in hematological malignancies including myelodysplastic syndrome, chronic myeloid leukemia, AML, and lymphoma (41, 42).

C-MYC is another oncoprotein that accelerates cell proliferation, and its de-regulated expression has been reported in various cancers such as osteosarcoma, glioblastoma, and melanoma, and breast, colon, cervical, and lung carcinomas (43). In addition, activation of *C-MYC* by oncoprotein Tax is associated with poor prognosis in acute and lymphomatous types of ATLL (44).

For the first time, current findings indicated significant down-regulation of BMI-1 by parthenolide, and this effect was more considerable after our combinatorial treatment. Decreased expression of *C-MYC*, however, was only observed upon single-use of ATO, which is in line with reports that showed *C-MYC* down-regulation after ATO treatment of mantle cell lymphoma and lung cancer cells (45, 46).

Conclusion

The present study provided evidence, for the first time, on combinatorial effects of parthenolide and ATO in ATLL cells. Since chemotherapy resistance is a major challenge in the treatment of ATLL, parthenolide could serve as a potent agent to improve the efficacy of current therapeutics. Despite great pharmacological properties of parthenolide, poor water-solubility of this compound caused limitations in clinical trials. Certainly, more research is necessary to clarify mechanisms of parthenolide action in different combinatorial

strategies, before translating it to the clinical setting.

Acknowledgment

The results presented in this paper were part of a student thesis. This work was supported by a grant from Mashhad University of Medical Sciences (no. 941052).

Conflicts of Interest

The authors declare that there are no conflicts of interest.

References

- Martin JL, Maldonado JO, Mueller JD, Zhang W, Mansky LM. Molecular studies of HTLV-1 replication: An update. *Viruses*. 2016; 8:31-37.
- Utsunomiya A, Choi I, Chihara D, Seto M. Recent advances in the treatment of adult T-cell leukemia-lymphomas. *Cancer Sci*. 2015; 106:344-351.
- Yared JA, Kimball AS. Optimizing management of patients with adult T cell leukemia-lymphoma. *Cancers (Basel)*. 2015; 7:2318-2329.
- Bittencourt AL, Vieira MdG, Brites CR, Farre L, Barbosa HS. Adult T-cell leukemia/lymphoma in Bahia, Brazil: analysis of prognostic factors in a group of 70 patients. *Am J Clin Pathol*. 2007; 128:875-882.
- Ishitsuka K, Tamura K. Human T-cell leukaemia virus type I and adult T-cell leukaemia-lymphoma. *Lancet Oncol*. 2014; 15:e517-e526.
- Kchour G, Tarhini M, Kooshyar M-M, El Hajj H, Wattel E, Mahmoudi M, et al. Phase 2 study of the efficacy and safety of the combination of arsenic trioxide, interferon alpha, and zidovudine in newly diagnosed chronic adult T-cell leukemia/lymphoma (ATL). *Blood*. 2009; 113:6528-6532.
- Bazarbachi A, Suarez F, Fields P, Hermine O. How I treat adult T-cell leukemia/lymphoma. *Blood*. 2011; 118:1736-1745.
- Parada-Turska J, Paduch R, Majdan M, Kandefer-Szerszeń M, Rzeski W. Antiproliferative activity of parthenolide against three human cancer cell lines and human umbilical vein endothelial cells. *Pharmacol Rep*. 2007; 59:233.
- Dey S, Sarkar M, Giri B. Anti-inflammatory and anti-tumor activities of parthenolide: an update. *J Chem Biol Ther*. 2016; 2:1-6.
- Taleghani A, Nasser MA, Iranshahi M. Synthesis of dual-action parthenolide prodrugs as potent anticancer agents. *Bioorg Chem*. 2017; 71:128-134.
- Hayashi S, Koshiba K, Hatashita M, Sato T, Jujo Y, Suzuki R, et al. Thermosensitization and induction of apoptosis or cell-cycle arrest via the MAPK cascade by parthenolide, an NF- κ B inhibitor, in human prostate cancer androgen-independent cell lines. *Int J Mol Med*. 2011; 28:1033-1042.
- Liu JW, Cai MX, Xin Y, Wu QS, Ma J, Yang P, et al. Parthenolide induces proliferation inhibition and apoptosis of pancreatic cancer cells *in vitro*. *J Exp Clin Cancer Res*. 2010; 29:108.
- Zhang S, Ong C-N, Shen H-M. Critical roles of intracellular thiols and calcium in parthenolide-induced apoptosis in human colorectal cancer cells. *Cancer Lett*. 2004; 208:143-153.
- Suvannasankha A, Crean CD, Shanmugam R, Farag SS, Abonour R, Boswell HS, et al. Antimyeloma effects of a sesquiterpene lactone parthenolide. *Clin Cancer Res*. 2008; 14:1814-1822.
- Carlisi D, Lauricella M, D'Anneo A, Buttitta G, Emanuele S, Di Fiore R, et al. The synergistic effect of SAHA and parthenolide in MDA-MB231 breast cancer cells. *J Cell Physiol*. 2015; 230:1276-1289.
- Kim S-L, Kim SH, Trang KTT, Kim IH, Lee S-O, Lee ST, et al. Synergistic antitumor effect of 5-fluorouracil in combination with parthenolide in human colorectal cancer. *Cancer Lett*. 2013; 335:479-486.
- Chou T, Martin N. CompuSyn software for drug combinations and for general dose-effect analysis, and user's guide. Paramus: ComboSyn Inc 2007.
- Kato S, Nishimura J, Muta K, Yufu Y, Nawata H, Ideguchi H. Overexpression of P-glycoprotein in adult T-cell leukaemia. *Lancet*. 1990; 336:573.
- Sohma I, Fujiwara Y, Sugita Y, Yoshioka A, Shirakawa M, Moon J-H, et al. Parthenolide, an NF- κ B inhibitor, suppresses tumor growth and enhances response to chemotherapy in gastric cancer. *Cancer Genom Proteom*. 2011; 8:39-47.
- Wozniak M, Szulawska-Mroczek A, Hartman ML, Nejc D, Czyz M. Parthenolide complements the cell death-inducing activity of doxorubicin in melanoma cells. *Anticancer Res*. 2013; 33:3205-3212.
- Zhang D, Qiu L, Jin X, Guo Z, Guo C. Nuclear factor- κ B inhibition by parthenolide potentiates the efficacy of taxol in non-small cell lung cancer *in vitro* and *in vivo*. *Mol Cancer Res*. 2009; 7:1139-1149.
- Liu D, Liu Y, Liu M, Ran L, Li Y. Reversing resistance of multidrug-resistant hepatic carcinoma cells with parthenolide. *Future Oncol*. 2013; 9:595-604.
- Trang KTT, Kim S-L, Park S-B, Seo S-Y, Choi C-H, Park J-K, et al. Parthenolide sensitizes human colorectal cancer cells to tumor necrosis factor-related apoptosis-inducing ligand through mitochondrial and caspase dependent pathway. *Intestinal Res*. 2014; 12:34-41.
- Park WH, Seol JG, Kim ES, Hyun JM, Jung CW, Lee CC, et al. Arsenic trioxide-mediated growth inhibition in MC/CAR myeloma cells via cell cycle arrest in association with induction of cyclin-dependent kinase inhibitor, p21, and apoptosis. *Cancer Res*. 2000; 60:3065-3071.
- Ralstin MC, Gage EA, Yip-Schneider MT, Klein PJ, Wiebke EA, Schmidt CM. Parthenolide cooperates with NS398 to inhibit growth of human hepatocellular carcinoma cells through effects on apoptosis and G0-G1 cell cycle arrest. *Mol Cancer Res*. 2006; 4:387-399.
- Hoofd C, Wang X, Lam S, Jenkins C, Wood B, Giambra V, et al. CD44 promotes chemoresistance in T-ALL by increased drug efflux. *Exp Hematol*. 2016; 44:166-171.
- Koopman G, Heider K, Horst E, Adolf G, Van Den Berg F, Ponta H, et al. Activated human lymphocytes and aggressive non-Hodgkin's lymphomas express a homologue of the rat metastasis-associated variant of CD44. *J Exp Med*. 1993; 177:897-904.
- Ghaffari S, Dougherty G, Eaves A, Eaves C. Altered patterns of CD44 epitope expression in human chronic and acute myeloid leukemia. *Leukemia*. 1996; 10:1773-1781.
- Ghaffari S, Dougherty G, Lansdorp P, Eaves A, Eaves C. Differentiation-associated changes in CD44 isoform expression during normal hematopoiesis and their alteration in chronic myeloid leukemia. *Blood*. 1995; 86:2976-2985.
- Chagan-Yasutan H, Tsukasaki K, Takahashi Y, Oguma S, Harigae H, Ishii N, et al. Involvement of osteopontin and its signaling molecule CD44 in clinicopathological features of adult T cell leukemia. *Leukemia Res*. 2011; 35:1484-1490.
- Shih VF-S, Tsui R, Caldwell A, Hoffmann A. A single NF κ B system for both canonical and non-canonical signaling. *Cell Res*. 2011; 21:86-102.
- Rauch DA, Ratner L. Targeting HTLV-1 activation of NF κ B in mouse models and ATLL patients. *Viruses*. 2011; 3:886-900.
- Kim SL, Liu YC, Seo SY, Kim SH, Kim IH, Lee SO, et al. Parthenolide induces apoptosis in colitis-associated colon cancer, inhibiting NF- κ B signaling. *Oncol Lett*. 2015; 9:2135-2142.
- Kong FC, Zhang JQ, Zeng C, Chen WL, Ren WX, Yan GX, et

- al. Inhibitory effects of parthenolide on the activity of NF- κ B in multiple myeloma via targeting TRAF6. *J Huazhong Uni Sci Technol.* 2015; 35:343-349.
35. Kim S-L, Kim SH, Park YR, Liu Y-C, Kim E-M, Jeong H-J, *et al.* Combined parthenolide and balsalazide have enhanced antitumor efficacy through blockade of NF- κ B activation. *Mol Cancer Res.* 2017; 15:141-151.
36. Yip-Schneider MT, Nakshatri H, Sweeney CJ, Marshall MS, Wiebke EA, Schmidt CM. Parthenolide and sulindac cooperate to mediate growth suppression and inhibit the nuclear factor- κ B pathway in pancreatic carcinoma cells. *Mol Cancer Ther.* 2005; 4:587-594.
37. Dolcet X, Llobet D, Pallares J, Matias-Guiu X. NF- κ B in development and progression of human cancer. *Virchows Arch.* 2005; 446:475-482.
38. Jiang L, Li J, Song L. Bmi-1, stem cells and cancer. *Acta Biochim Biophys Sin.* 2009; 41:527-534.
39. Bhattacharya R, Mustafi SB, Street M, Dey A, Dwivedi SKD. Bmi-1: At the crossroads of physiological and pathological biology. *Genes Dis.* 2015; 2:225-239.
40. Wang MC, Li CL, Cui J, Jiao M, Wu T, Jing L, *et al.* BMI-1, a promising therapeutic target for human cancer. *Oncol Lett.* 2015; 10:583-588.
41. Molofsky AV, He S, Bydon M, Morrison SJ, Pardoll R. Bmi-1 promotes neural stem cell self-renewal and neural development but not mouse growth and survival by repressing the p16Ink4a and p19Arf senescence pathways. *Genes Dev.* 2005; 19:1432-1437.
42. Bhattacharyya J, Mihara K, Ohtsubo M, Yasunaga Si, Takei Y, Yanagihara K, *et al.* Overexpression of BMI-1 correlates with drug resistance in B-cell lymphoma cells through the stabilization of survivin expression. *Cancer Sci.* 2012; 103:34-41.
43. Pelengaris S, Khan M, Evan G. c-MYC: more than just a matter of life and death. *Nat Rev Cancer.* 2002; 2:764-776.
44. Mihashi Y, Mizoguchi M, Takamatsu Y, Ishitsuka K, Iwasaki H, Koga M, *et al.* C-MYC and its main ubiquitin ligase, FBXW7, influence cell proliferation and prognosis in adult T-cell leukemia/lymphoma. *Am J Surg Pathol.* 2017; 41:1139-1149.
45. Li XY, Li Y, Zhang L, Liu X, Feng L, Wang X. The antitumor effects of arsenic trioxide in mantle cell lymphoma via targeting Wnt/ β -catenin pathway and DNA methyltransferase-1. *Oncol Rep.* 2017; 38:3114-3120.
46. HE XI, HU CI, MA BI. The effect of arsenic trioxide in human lung adenocarcinoma A549 cell line proliferation and c-Myc gene expression. *J Yanan Uni.* 2013; 2:4-7.